Fano phase resonances in multilayer metal-dielectric compound gratings

Isroel M. Mandel
Department of Physics, Graduate Center, City College of the City University of New York, New York, New York 10031, USA

Andrii B. Golovin
Center for Metamaterials, City College of the City University of New York, New York, New York 10031, USA

David T. Crouse*
Department of Electrical Engineering, The City College of New York, New York, New York 10031, USA
(Received 22 January 2013; published 30 May 2013)

Phase resonances in multilayer metal-dielectric compound gratings are numerically modeled and described. Additional grating layers allow for more complex types of phase resonances in which light travels in different, circuitous routes through the structure. It is shown that phase resonances produce highly enhanced fields, have a very narrow bandwidth, are Fano resonances with asymmetric line shapes of their reflectance, and produce a complete inversion in the transmittivity and opacity of low loss structures. Several multigrating structures are numerically modeled that show the addition of more complicated phase resonances as more layers are added to the structure. The dispersion curves of the multiple bands of phase resonances are predicted using an analytical approach and numerical modeling. Applications of the resonance effects are described for optical filters.

DOI: 10.1103/PhysRevA.87.053847 PACS number(s): 42.25.Fx, 41.20.Jb, 42.79.−e

I. INTRODUCTION

Resonant electromagnetic modes in single layer and multilayer metal-dielectric gratings exhibit enhanced and anomalous electromagnetic properties that have been extensively investigated in many past works [1–5]. In single layer gratings, anomalously enhanced optical transmission (EOT), produced either by surface plasmons or waveguide cavity modes, light harvesting, light trapping, and other complex optical phenomena have been observed [1,6–8]. Multilayer metal-dielectric gratings and hole arrays have also been shown to produce numerous interesting optical effects, including EOT, negative index of refraction, and slow and fast light modes [9,10]. Besides these optical modes, phase resonances (also called π resonances) are a type of Fano resonance that have been attracting more attention due to their unusual optical properties, including their effect of flipping the transmittivity and opacity of a film, producing light circulating modes, trapping and stopping light, producing negative dispersion and negative index of refraction, and electromagnetically induced transparency [8,11–18]. To date however, phase resonances have only been studied in single layer grating structures and not in multilayer gratings, yet such modes should occur in multilayer gratings in greater number and variety, and show a richer set of electromagnetic behavior.

Phase resonances (PRs) can occur due to the coupling of *s*- or *p*-polarized waveguide cavity modes (WCMs) in compound transmission gratings (CTGs), i.e., gratings with more than one *dissimilar* groove per repeating unit cell, as shown in Fig. 1 [8,19]. The dissimilar grooves within the unit cell can be different either by having different widths, different dielectric filling materials, or some other difference that breaks the mirror symmetry about a plane in the middle of, and equidistant from, the two grooves in the unit cell. At particular frequencies within the bandwidth of the WCMs supported by the grooves, WCMs can be excited that have highly enhanced fields compared to the incident beam, and with the WCMs in the grooves within the unit cell having a well defined relative phase difference [π radians for CTGs with two dissimilar grooves in the unit cell (i.e., a two-groove CTG)]; this resonantly coupled mode is a PR. In Ref. [20], Mandel *et al.* derived the relationship between frequencies, momenta, structural dimensions, and materials parameters (i.e., the dispersion curve) of PRs in two-groove CTGs. In Ref. [19], Bendoym *et al.* theoretically showed that PRs in low loss two-groove CTGs can provide arbitrarily high field enhancement of the incident beam (limited only by the optical loss in the materials and fabrication tolerances) and electromagnetic filtering and channeling capabilities that may be useful for corrugated surface antennas. Also, the reader is referred to Ref. [18] that describes the design, fabrication, and characterization of two single layer grating structures that support either *s*- or *p*-polarized PRs; the experimental results matched the numerically modeled results as well as the predictions of the analytical model developed in Ref. [20].

II. ELECTROMAGNETIC MODES IN MULTILAYER GRATINGS

The type of structure that will be studied in this work is shown in Fig. 1, which shows a multilayer grating (MLG) with N total layers and $P = (N - 1)/2$ grating layers; thus there are $(N + 1)/2$ homogeneous dielectric layers, two of which are the semi-infinite substrate and superstrate. Many different structures are possible, with multiple dissimilar grooves in the unit cell in each grating layer, different lateral offsets of each grating layer, and with dissimilar dielectric spacer layers between the grating layers. But in this work, the structures that are considered have only two dissimilar grooves (per grating layer) within the unit cell, all the grating layers are identical and are vertically aligned, the dielectric spacer layers all have the same thickness and dielectric constant, and the dielectric

*dcrouse@ccny.cuny.edu

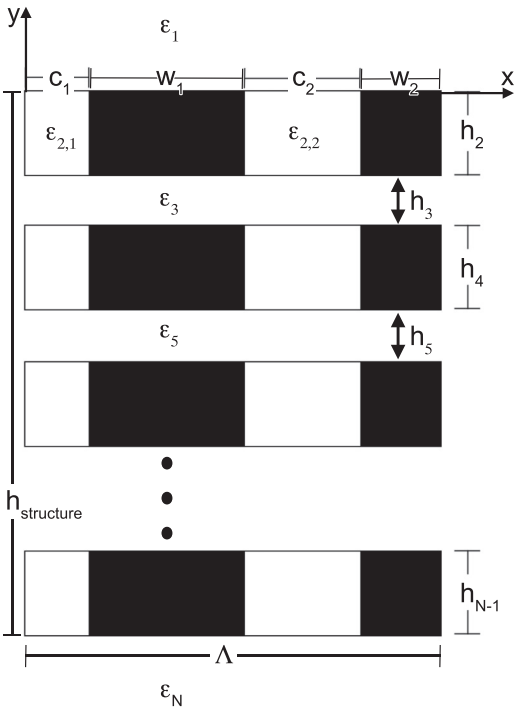

FIG. 1. The multilayer grating structure studied in this work. The P grating layers are separated by $P-1$ homogeneous dielectric spacer layers. The unit cell has two slightly dissimilar grooves in the unit cell of period Λ. The grating layers are vertically aligned such that the grooves form two straight columns of grooves.

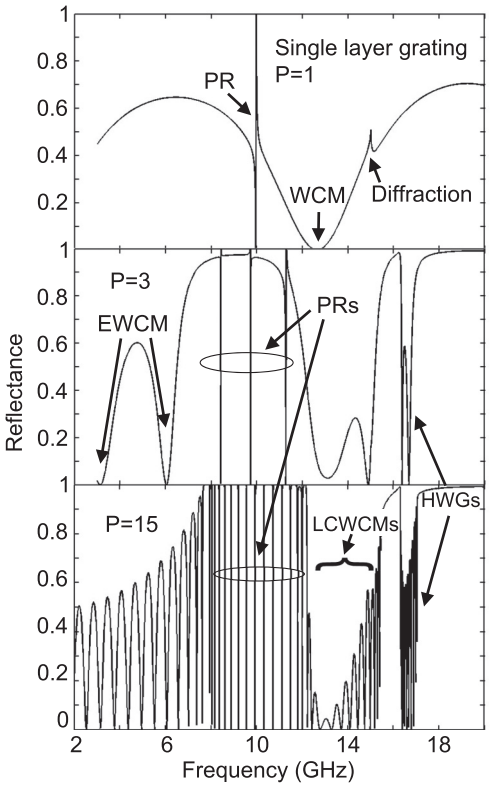

FIG. 2. The reflectance for three MLG structures with $P=1$ (top), $P=3$ (center), and $P=15$ (bottom) grating layers. The single layer grating (top) has the typical PR with the asymmetrical line shape, a broad WCM, and the Rayleigh anomaly at 15 GHz associated with diffraction. The two MLGs (center and bottom) have additional PRs, three PRs for the $P=3$ MLG and 15 PRs for the $P=15$ MLG.

constant of the superstrate and substrate is 1. Figure 2 shows the normal incident reflectance for a structure with different numbers of grating layers $P=1$ [i.e., the single layer grating (SLG)], $P=3$, and $P=15$. The particular structure studied here has a period of $\Lambda=20$ mm (the unit cell includes *both* grooves 1 and 2), $h_g=10$ mm thick (with $g=2,4,\ldots$), with metals that are perfect electrical conductors (PECs), groove 1 has a width of $c_1=3$ mm, and groove 2 has a width of $c_2=3.67$ mm; both grooves have $\epsilon_g=1$, and with $w_1=6$ mm and $w_2=7.34$ mm. The superstrate, substrate, and homogeneous spacer layers are vacuum and the spacer layers all have a thickness of 3.334 mm. All the results were obtained by using the rigorous coupled wave analysis, and verified by using COMSOL, a finite element frequency domain solver.

For the structure with only one grating layer, the reflectance shows the effects of several electromagnetic resonance modes. There is a p-polarized WCM at 12.65 GHz that channels all the incident light through the two grooves and into the substrate; this type of EOT has been described in many past works [6–8]. There also is a Rayleigh anomaly due to the onset of far-field diffraction modes at 15 GHz. Also, there is a PR at 9.955 GHz exhibiting all the typical features of PRs (e.g., Fano resonance type of line shape, flipping of the transmittivity and opacity, and light circulation) that have been extensively discussed in past works [18–20].

Additional grating layers can be added to the structure in different ways, however, let us first add additional grating layers in a simple way, namely, add identical grating layers with identical dielectric spacing layers and have them vertically aligned with each other (as shown in Fig. 1). Figure 2 shows the specular reflection from three structures with 1, 3, and 15 grating layers. For the $P=3$ structure, four new optical features are seen: additional PRs, new WCMs at lower frequencies, the original WCM acquiring multiple dips and peaks, and other higher energy PRs associated with the cavities formed by the dielectric layers between vertically aligned and vertically spaced wires.

First, one can identify a group of WCMs in the MLG that is associated with the original WCM of the SLG; they have similar frequencies, and the fields of the WCMs are confined to single grooves in each grating layer. However, this original WCM of the SLG is modified in the MLG because the WCMs along each vertical column of grooves can form a linear combination of waveguide cavity modes (i.e., LCWCMs), with the WCMs being excited with equal amplitude but with a difference in phase (see Fig. 3), i.e., the series of WCMs have acquired a nonzero k_y (similar to molecular orbitals in linear combination of atomic orbitals). There are $P-1$ of these modes (each with a different frequency) for a MLG with P grating layers. The highest (lowest) energy LCWCMs is a state with the fields of the WCMs in two vertically neighboring grooves being exactly in phase (out of phase) with each other. This phase difference is along each column of grooves and the two columns of grooves have identically excited WCMs, thus

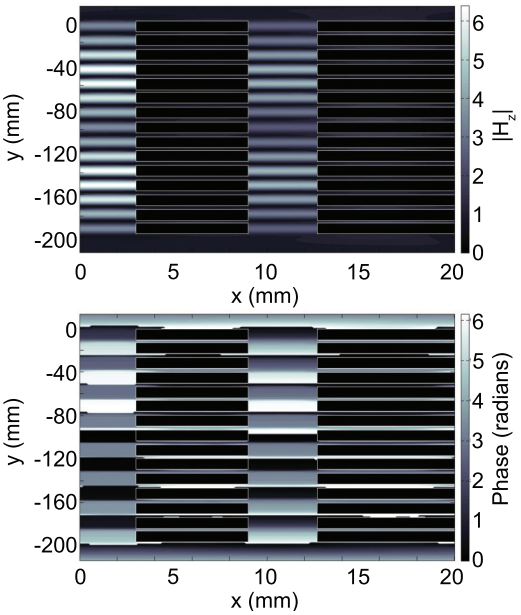

FIG. 3. (Color online) A cross section of $P = 15$ MLG showing $|H_z|$ for the lowest energy LCWCM (12.239 GHz) (top) and the phase of H_z (bottom) excited by a normal incident plane wave from above. All of the $P - 1$ LCWCMs have similar field profiles in that H_z is largely confined to each individual groove as opposed to what occurs with EWCMs. However, the phase of the fields in the vertically neighboring grooves can vary from π radians for the lowest energy LCWCM (shown in the bottom plot) to 0 radians for the highest energy LCWCM (not shown). The bottom plot shows the phase of the 12.239 GHz LCWCM, showing that the fields of the WCMs in vertically adjacent grooves are π radians out of phase; note that 0 radians (in black) yields the same phase as 2π radians (in white) and that gray corresponds to a π radians phase.

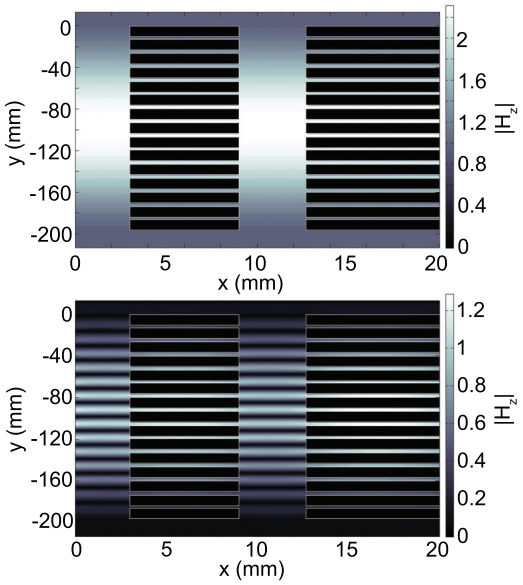

FIG. 4. (Color online) A cross section of $P = 15$ MLG showing $|H_z|$ for the lowest energy EWCM (0.63 GHz) (top) and highest energy EWCM (7.616 GHz) (bottom) excited by a normal incident plane wave from above (i.e., $k_x = 0$). It is seen that the vertical column of grooves acts like a single waveguide, allowing the field to spread out along the entire thickness of the structure (i.e., $h_{\text{structure}}$) for the lowest energy EWCM and have progressively higher energies for EWCMs with a progressively larger number of nodes in the field along the vertical extent of the structure.

these modes are not PRs or Fano resonances, and the further description of these modes is not within the scope of this work.

As for the new WCMs at lower frequencies, they are produced by the grooves in each grating layer coupling with the identical (structurally and compositionally) grooves above and below them, making for an effectively deeper groove that has a thickness equal to the entire thickness of the structure ($h_{\text{structure}}$); these new WCMs are labeled as extended waveguide cavity modes (EWCMs), and there are $P - 1$ of these modes for a MLG with P grating layers (see Fig. 4). EWCMs exist with or without the occurrence of PRs and can be used to lower the loss within optical gratings by lowering the surface area of lossy metal encountered by the fields of the WCMs.

The main focus of this paper however, is the new types of PRs that can exist in MLG structures. The first and most obvious type is the same type that occurs in a single layer grating. More specifically, the resonances with H_z in the two grooves of the unit cell (or, as will be seen later, groups of vertical grooves) having a π radians phase difference, as shown in Fig. 5. The Poynting vector profile is shown in Fig. 6. The vertically stacked grooves in the multiple layers allow the fields to couple with each other in ways not possible in SLGs.

For a structure with P grating layers, the highest energy PR has P nodes along the vertical stack of grooves, i.e., H_z in each groove is π radians out of phase with H_z in the groove above it, below it, to its right and left [Fig. 5 (top)]. For this highest energy PR mode, the net energy flow is back and forth one time between the two vertical stacks of grooves via the horizontal waveguides (HWGs) connecting the two columns of grooves (Fig. 6). The lowest energy mode has one node for H_z that is spread throughout the vertical extent of the structure, and with H_z in the two vertical columns of grooves in the unit cell being approximately π radians out of phase relative to each other [Fig. 5 (bottom)], and the net energy flow making P back and forth journeys between the two columns of grooves (Fig. 7). There are $P - 2$ other PRs with intermediate energies for a total of P PRs for a structure with P grating layers.

The line shapes of the reflectance for MLGs with a large number of layers have the following properties. One property is that off resonance, the baseline reflectance goes to unity as the number of grating layers increases, indicating an optical stop band or band gap of the structure. This band gap would be "defect" free (i.e., no transmission states) if all the grooves in all the layers are identical; but the PRs in the multilayer CTG structure produce defect states that allow for light within a narrow bandwidth to be transmitted through the structure. The second property of the line shape is more apparent if one zooms into the reflectance curve at each PR; the line shape is still best described as a Fano resonance with an asymmetry parameter $q = 1$ [21] with the reflectance curve going from close to unity to zero for increasing frequency on the low frequency side of the PR, then going to exactly unity (for lossless structures) on the high frequency side and then decreasing back to a baseline

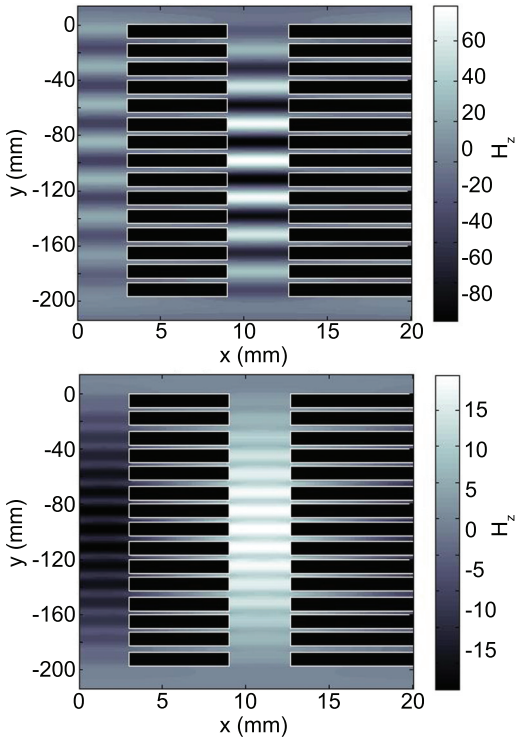

FIG. 5. (Color online) A cross section of $P = 15$ MLG showing H_z for the highest energy PR (11.996 GHz) (top) and lowest energy PR (7.941 GHz) (bottom) excited by a normal incident plane wave from above. It is seen that the vertical stacks of grooves couple, allowing for the fields of the PRs to spread out vertically along the entire thickness of the structure (as is seen in the lowest energy mode). With each of these PRs, the energy flows from one vertical stack to the other via the horizontal grooves between the metal wires formed by the dielectric spacer layers (Figs. 6 and 7).

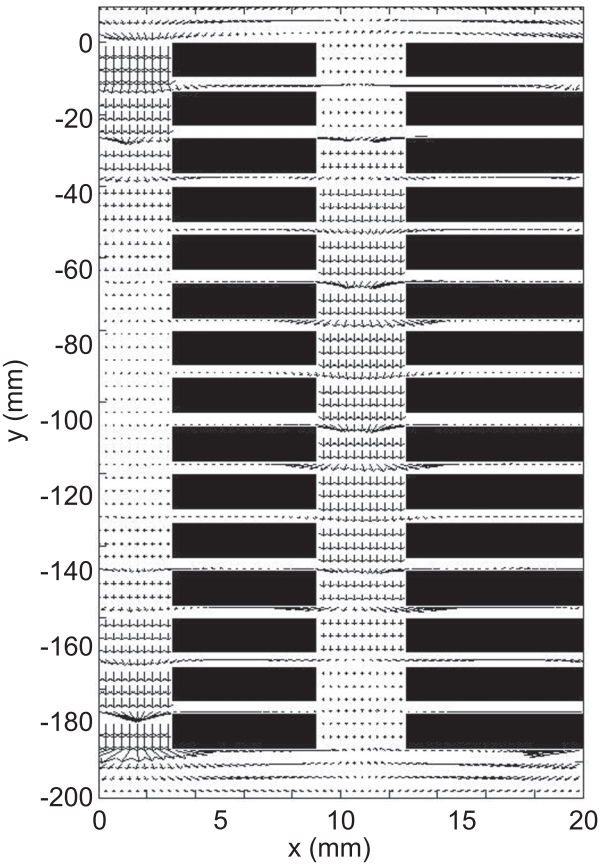

FIG. 6. The Poynting vector profile for the 11.996 GHz PR in the $P = 15$ MLG structure, excited by a normal incident beam from above. The energy of this highest energy PR flows in a similar way to the 7.941 GHz PR but has progressively lesser amounts of weaving back and forth between the two columns of grooves.

level. The high baseline reflectance (i.e., off resonance) and narrow bandwidth unity transmittance at the frequency of the PR leads one to consider such structures for use as notch filters, as was done in Ref. [19].

III. DISPERSION CURVES OF MULTILAYER GRATINGS

The ω-k diagram of the MLG with three grating layers is shown in Fig. 8. The dispersion curve of the PRs in this MLG have the same properties as the dispersion curve of the PR band in the SLG. In Ref. [20], Mandel *et al.* derived the dispersion relation for PRs in a slightly perturbed single layer lamellar grating structure, with two only slightly dissimilar grooves in the unit cell, to produce a CTG that supports PRs with frequencies ω_{pr} and momenta (k_x) for which the following equation is satisfied:

$$\frac{2i\gamma_0}{\epsilon_g}\tan\left(\frac{\gamma_0 h_g}{2}\right) = \frac{\beta_1\beta_{-1}(\Lambda/\epsilon_s w)}{\beta_1 \mathrm{sinc}^2\left(\alpha_{-1}\frac{w}{2}\right) + \beta_{-1}\mathrm{sinc}^2\left(\alpha_1\frac{w}{2}\right)} \qquad (1)$$

with $\beta_{\pm 1} = (\epsilon_s k_o^2 - \alpha_{\pm 1}^2)^{1/2}$, $\alpha_{\pm 1} = k_x \pm K$, $\gamma_0 = \sqrt{\epsilon_g} k_o$, and $k_o = \omega_{pr}/c$, where $K = 2\pi/\Lambda$, Λ is the period of the two-groove CTG (i.e., the length of the unit cell that contains *both* grooves), ϵ_s is the dielectric constant of the superstrate and substrate (both are assumed to be composed of the same material), h_g is the height of the grooves, w and ϵ_g are the widths and dielectric constants, respectively, of both the grooves before the perturbation is introduced in either of these two values, and the sinc function is $\mathrm{sinc}(x) = \sin(x)/x$. The solutions of Eq. (1) for ω_{pr} for a range of k_x values can be obtained to yield the full dispersion curve of PRs in two-groove CTGs.

While there is only one band of PRs for SLGs, MLGs support P bands of PRs. These multiple bands arise due to the ability of the WCMs in vertically stacked grooves to couple. It is seen in Fig. 2 that as one goes from the $P = 1$ SLG to the $P = 3$ MLG, and then to a $P = 15$ MLG, new PRs occur over a range of frequencies with the center frequency provided by Eq. (1); this occurs because the fields of the PRs are more confined in the y direction (for higher energy PRs) or less confined (for lower energy PRs) relative to the confinement of PRs in SLGs. It is apparent from studying Fig. 2 that the field variation along the vertical extent of the structure (i.e., the y direction) can be characterized by an effective k_y wave vector component that has the form $k_{y,m} = m\pi/h_{\text{structure}}$ where $m = 1 \cdots P$. This $k_{y,m}$ component can be combined with k_x and the energies of the PRs in MLGs can then be expressed

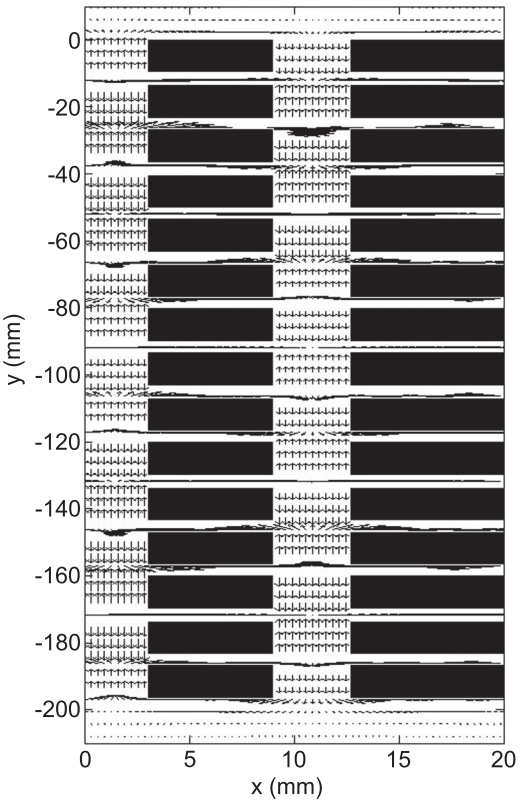

FIG. 7. The Poynting vector profile for the 7.941 GHz PR in the $P = 15$ MLG structure, excited by a normal incident beam from above. The lowest energy mode has the unusual property that the flow of energy in each vertical groove is in the opposite direction to that of the vertical grooves to its right, left, top, and bottom; thus energy is taking a long, circuitous route through the structure, weaving its way down a groove, turning and going down the horizontal groove between the wires and into the other column of grooves and repeating this process until it emerges from the structure and into the substrate.

as

$$\omega_m^2 = c^2\left[k_x(\omega)^2 + k_{y,m}^2\right] = c^2 k_x(\omega)^2 + \left(\frac{c\pi}{\sqrt{\epsilon_{\text{eff}}}h_{\text{structure}}}\right)^2\left(\frac{P^2}{2} - m^2\right) \quad (2)$$

with k_x being a function of ω [given by Eq. (1)], and ϵ_{eff} being the effective dielectric constant of the structure as experienced by the PRs. The value of ϵ_{eff} can be approximated by $\{\lambda/[2(h_{\text{grating}} + h_{\text{spacer}})]\}^2$ where λ is the center wavelength within the bandwidth at which PRs occur; for the structure studied in this work, $\epsilon_{\text{eff}} \simeq 56$. Also, the integer m only varies from 1 to only P where P is the number of grating layers. One may obtain an approximation for the frequency of the midpoint of the range in which PRs occur from Eq. (1) and then use Eq. (2) to find the spacings between any two other PR bands:

$$\omega_m^2 - \omega_{m-1}^2 = \left(\frac{c\pi}{\sqrt{\epsilon_{\text{eff}}}h_{\text{structure}}}\right)^2[m^2 - (m-1)^2]. \quad (3)$$

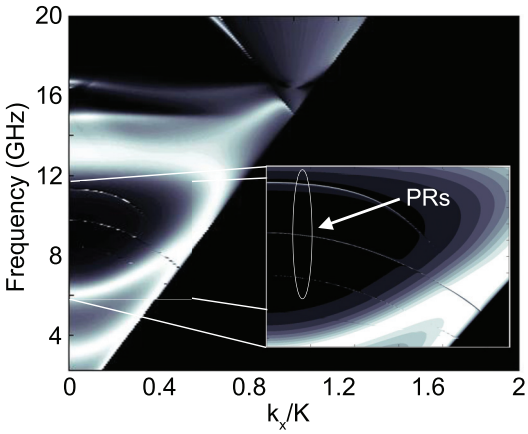

FIG. 8. (Color online) The ω-k diagram showing the *transmittance* as a function of in-plane momentum and frequency for the $N = 7$ ($P = 3$) MLG. Because there are three grating layers, there will be three narrow bands of PRs with frequency spacings predicted by Eq. (3). Black (white) corresponds to low (high) transmission.

There are other PRs and Fano resonances that occur in the grating shown in Fig. 1. For the structure studied in this work, the reflectance dips between 16 and 17 GHz do not have an asymmetric line shape and are due to the excitation of coupled HWG modes formed in the dielectric spacer layer between the vertically aligned and vertically separated metal wires of two grating layers. However, for other MLG structures, it has been observed that two WCMs in two vertically neighboring HWGs can have H_z with a π radians relative phase difference, and the reflectance curves can have an asymmetric line shape or other line shapes indicative of a Fano resonance [21]—all the markings of a PR. Yet these structures that support PRs composed of coupled HWGs are encountered much more rarely and thus will not be discussed in detail in this work.

IV. CONCLUSION

It was shown in this work that new types of phase resonances, a type of Fano resonance, occur in multilayer compound grating structures that do not occur in single layer compound gratings. The PR band that occurs in a single layer compound grating is replicated with predictable energy differences between the bands in a multilayer structure, with one PR band for each grating layer in the structure. The flow of energy for these PRs shows a circuitous route through the structure, weaving back and forth between the vertical columns of grooves. In combination with our past works on phase resonances in single layer gratings that described the time dependent optical properties [19], the development of an analytical theory of phase resonances [20], and experimental verification of the modes [18], a comprehensive understanding of PRs is developing. Future work on the phase resonances in multilayer gratings will focus on the use of such structures for passive and actively tunable antennas and multiwavelength notch filters. An additional application that will be investigated is the use of PRs for highly sensitive chemical and biological sensors. In this application, a fluid or gas potentially containing toxins is allowed to flow through every other groove in a

single or multilayer grating structure. If the toxins are present, they will bind with highly specific binding agents that have been deposited on the walls of the groove, thus perturbing the permittivity of these grooves. The structure can then support PRs that will flip the transmissvity and opacity of the structure, leading to a detectable signal.

ACKNOWLEDGMENTS

This work is supported by the NSF Industry/University Cooperative Research Center for Metamaterials (Grant No. IIP-1068028) and by the AFOSR Bioenergy project (Grant No. FA9550-10-1-0350).

[1] T. W. Ebbesen, H. J. Lezec, H. F. Ghaemil, T. Thiol, and P. A. Wolff, Nature (London) **391**, 667 (1998).
[2] Z. Fan, L. Zhan, X. Hu, and Y. Xia, Opt. Commun. **281**, 5467 (2008).
[3] E. Popov, N. Bonod, M. Nevière, H. Rigneault, P.-F. Lenne, and P. Chaumet, Appl. Opt. **44**, 2332 (2005).
[4] H. Liu and P. Lalanne, Nature (London) **452**, 728 (2008).
[5] Q. Cao and P. Lalanne, Phys. Rev. Lett. **88**, 057403 (2002).
[6] D. Crouse, IEEE Trans. Electron Devices **52**, 2365 (2005).
[7] D. Crouse and P. Keshavareddy, Opt. Express **15**, 1415 (2007).
[8] D. Crouse, E. Jaquay, A. Maikal, and A. P. Hibbins, Phys. Rev. B **77**, 195437 (2008).
[9] M. R. Gadsdon, J. Parsons, and J. R. Sambles, J. Opt. Soc. Am. B **26**, 734 (2009).
[10] A. P. Hibbins, J. R. Sambles, C. R. Lawrence, and J. R. Brown, Phys. Rev. Lett. **92**, 143904 (2004).
[11] M. Beruete, M. Navarro-Ćia, M. Sorolla, and D. C. Skigin, Opt. Express **18**, 23957 (2010).
[12] R. A. Depine, A. N. Fantino, S. I. Grosz, and D. C. Skigin, Optik (Jena) **118**, 42 (2007).
[13] H. J. Rance, O. K. Hamilton, J. R. Sambles, and A. P. Hibbins, Appl. Phys. Lett. **95**, 041905 (2009).
[14] A. P. Hibbins, I. R. Hooper, M. J. Lockyear, and J. R. Sambles, Phys. Rev. Lett. **96**, 257402 (2006).
[15] M. Navarro-Cia, D. C. Skigin, M. Beruete, and M. Sorolla, Appl. Phys. Lett. **94**, 091107 (2009).
[16] D. C. Skigin and R. A. Depine, Phys. Rev. E **74**, 046606 (2006).
[17] D. C. Skigin and R. A. Depine, Opt. Commun. **262**, 270 (2006).
[18] A. Enemuo, M. Nolan, Y. Uk Jung, A. B. Golovin, and D. T. Crouse, J. Appl. Phys. **113**, 014907 (2013).
[19] I. Bendoym, A. B. Golovin, and D. T. Crouse, Opt. Express **20**, 22830 (2012).
[20] I. M. Mandel, A. B. Golovin, and D. T. Crouse, Phys. Rev. A **87**, 053833 (2013).
[21] A. Miroshnichenko, S. Flach, and Y. Kivshar, Rev. Mod. Phys. **82**, 2257 (2010).